DESY 11–115 ISSN 0418–9833
NSF–KITP–11–119

Single jet and prompt-photon inclusive production with multi-Regge kinematics: From Tevatron to LHC

B.A. Kniehl*

Kavli Institute for Theoretical Physics, Kohn Hall,

University of Santa Barbara, CA 93106, USA

V.A. Saleev†

Samara State University, Ac. Pavlov, 1, 443011, Samara, Russia and

S.P. Korolyov Samara State Aerospace University,

Moscow highway, 34, 443086, Samara, Russia

A.V. Shipilova‡

Samara State University, Ac. Pavlov, 1, 443011, Samara, Russia

E.V. Yatsenko§

II. Institut für Theoretische Physik, Universität Hamburg,

Luruper Chaussee 149, 22761 Hamburg, Germany

arXiv:1107.1462v2 [hep-ph] 7 Sep 2011

Abstract

We study single jet and prompt-photon inclusive hadroproduction with multi-Regge kinematics invoking the hypothesis of parton Reggeization in t-channel exchanges at high energy. In this approach, the leading contributions are due to the fusion of two Reggeized gluons into a Yang-Mills gluon and the annihilation of a Reggeized quark-antiquark pair into a photon, respectively. Adopting the Kimber-Martin-Ryskin and Blümlein prescriptions to derive unintegrated gluon and quark distribution functions of the proton from their collinear counterparts, for which we use the Martin-Roberts-Stirling-Thorne set, we evaluate cross section distributions in transverse momentum (p_T) and rapidity. Without adjusting any free parameters, we find good agreement with measurements by the CDF and D0 Collaborations at the Tevatron and by the ATLAS Collaboration at the LHC in the region $2p_T/\sqrt{S} \lesssim 0.1$, where $\sqrt{S}$ is the hadronic c.m. energy.

PACS numbers: 12.39.St, 12.40.Nn, 13.85.Qk, 13.87.Ce

*On leave of absence from II. Institut für Theoretische Physik, Universität Hamburg, Luruper Chaussee 149, 22761 Hamburg, Germany; Electronic address: kniehl@desy.de

†Electronic address: saleev@ssu.samara.ru

‡Electronic address: alexshipilova@ssu.samara.ru

§Electronic address: elena.yatsenko@desy.de

I. INTRODUCTION

The study of jet and prompt-photon inclusive production at high-energy colliders, such as the Fermilab Tevatron and the CERN LHC, is of great interest because it allows us to test perturbative quantum chromodynamics (QCD) and to extract information on the parton distribution functions (PDFs) of the proton. The presence of a jet or a photon with large transverse momentum, $p_T \gg \Lambda_{\rm QCD}$, with $\Lambda_{\rm QCD}$ being the asymptotic scale parameter, guarantees that the strong coupling constant remains small in the processes discussed here, i.e. typically $\alpha_s(p_T) \lesssim 0.1$.

The total collision energies, $\sqrt{S} = 1.8$ TeV and 1.96 TeV in Tevatron runs I and II, respectively, and $\sqrt{S} = 7$ TeV or 14 TeV at the LHC, sufficiently exceed the characteristic scale μ of the relevant hard processes, which is of order of p_T, *i.e.* we have $\Lambda_{\rm QCD} \ll \mu \ll \sqrt{S}$. In this high-energy regime, the contribution of partonic subprocesses involving t-channel parton (gluon or quark) exchanges to the production cross section can become dominant. Then the transverse momenta of the incoming partons and their off-shell properties can no longer be neglected, and we deal with "Reggeized" t-channel partons. If the particles produced in the collision are strongly separated in rapidity, they obey multi-Regge kinematics (MRK). If the same situation is realized with groups of particles, then quasi-multi-Regge kinematics (QMRK) is at work. In the case of single jet or prompt-photon inclusive production, this means the following: A single jet or a prompt photon is produced in the central region of rapidity, while other particles are produced with large modula of rapidities. In the experiment, the requirement of separation in rapidity can be controlled by the so-called isolation cone condition.

Previously, in Ref. [1], single jet inclusive production was studied in the Regge limit of QCD using the Balitsky-Fadin-Kuraev-Lipatov (BFKL) framework [2], and it was shown that the discrepancy between data and theory in the region of small values of $x_T = 2p_T/\sqrt{S}$ may be accounted for by the BFKL Pomeron. However, Pomeron exchange should be a dominant mechanism only at asymptotically large energies. In fact, in the energy range of the Tevatron and the LHC, the mechanism of Reggeized gluon and quark exchange should be more adequate.

Later, in Ref. [3], the infrared-stable single jet inclusive cross section was calculated at next-to-leading order (NLO) in the framework of high-energy factorization using the

unintegrated gluon PDF of the asymptotic BFKL approach and the one simply obtained by differentiating the collinear one w.r.t. the scale parameter, in compliance with BFKL evolution. The scatterings of off-shell partons were described by generalized cross sections calculated in the QMRK approach [4]. In contrast to the case of collinear factorization, NLO corrections were found to diminish the single jet inclusive cross section in the framework of high-energy factorization. However, in Ref. [3], the region of very small jet transverse momentum, $p_T < 20$ GeV, was analyzed, which lies far below the p_T range studied experimentally at the Tevatron and the LHC, $p_T > 50$ GeV, so that the predictions of Ref. [3] cannot be tested. Also taking into account that the unintegrated gluon PDFs are so far not well constrained, we consider the result of Ref. [3] to be preliminary and approximate.

The parton Reggeization framework [4] is particularly appropriate for this kind of high-energy phenomenology. It is based on an effective quantum field theory implemented with the non-Abelian gauge-invariant action including fields of Reggeized gluons [5] and Reggeized quarks [6].

Recently, this approach was successfully applied to interpret the production of prompt photons [7], diphotons [8], charmed mesons [9], bottom-flavored jets [10], charmonia [11], and bottomonia [12] as measured at the Tevatron and at DESY HERA in the small-x_T regime. In this paper, we continue our work in the parton Reggeization framework by studying the distributions in transverse momentum and rapidity (y) of single jet and prompt-photon inclusive hadroproduction. We assume the MRK production mechanism to be the dominant one at small x_T values. We compare our results with experimental data taken by the CDF [13] and D0 [14–16] Collaborations at the Tevatron with $\sqrt{S} = 1.8$ TeV and 1.96 TeV and by the ATLAS Collaboration [17, 18] at the LHC with $\sqrt{S} = 7$ TeV. We also present predictions for the p_T and y distributions of single jet and prompt-photon inclusive production at the LHC with $\sqrt{S} = 14$ TeV.

II. BORN AMPLITUDES WITH MULTI-REGGE KINEMATICS

We examine single jet and prompt-photon inclusive production in proton-antiproton collisions at the Tevatron and in proton-proton collisions at the LHC. To leading order (LO) in the parton Reggeization framework, the relevant hard-scattering processes are $\mathcal{R} + \mathcal{R} \to g$ and $\mathcal{Q} + \overline{\mathcal{Q}} \to \gamma$, where $\mathcal{R}$ is a Reggeized gluon, g is a Yang-Mills gluon, $\mathcal{Q}$ is a Reggeized

quark, and γ is a photon. Working in the center-of-mass (c.m.) frame, we write the four-momenta of the incoming hadrons as $P^\mu_{1,2} = (\sqrt{S}/2)(1,0,0,\pm 1)$ and those of the Reggeized partons as $q_i^\mu = x_i P_i^\mu + q_{iT}^\mu$ $(i = 1, 2)$, where x_i are the longitudinal momentum fractions and $q_{iT}^\mu = (0, \mathbf{q}_{iT}, 0)$, with $\mathbf{q}_{iT}$ being transverse two-momenta, and we define $t_i = -q_{iT}^2 = \mathbf{q}_{iT}^2$. The gluon and photon produced in the $2 \to 1$ partonic subprocesses have four-momentum $p^\mu = q_1^\mu + q_2^\mu = (p^0, \mathbf{p}_T, p^3)$, with $\mathbf{p}_T^2 = t_1 + t_2 + 2\sqrt{t_1 t_2}\cos\phi_{12}$, where ϕ_{12} is the azimuthal angle enclosed between $\mathbf{q}_{1T}$ and $\mathbf{q}_{1T}$. Introducing the light-cone vectors $(n^\pm)^\mu = (1, 0, 0, \pm 1)$, we define $k^\pm = k \cdot n^\pm$ for any four-vector k^μ.

The Fadin-Kuraev-Lipatov effective $\mathcal{R}\mathcal{R}g$ vertex reads [2, 19]:

$$C^{g,\mu}_{\mathcal{R}\mathcal{R}}(q_1, q_2) = -\sqrt{4\pi\alpha_s} f^{abc} \frac{q_1^+ q_2^-}{2\sqrt{t_1 t_2}} \left[(q_1 - q_2)^\mu + \frac{(n^+)^\mu}{q_1^+} \left(q_2^2 + q_1^+ q_2^- \right) - \frac{(n^-)^\mu}{q_2^-} \left(q_1^2 + q_1^+ q_2^- \right) \right], \tag{1}$$

where α_s is the strong-coupling constant, a and b are the color indices of the Reggeized gluons with incoming four-momenta q_1 and q_2, and f^{abc} are the structure constants of the color group group SU(3). The squared amplitude of the partonic subprocess $\mathcal{R} + \mathcal{R} \to g$ is straightforwardly found from Eq. (1) to be

$$\overline{|\mathcal{M}(\mathcal{R} + \mathcal{R} \to g)|^2} = \frac{3}{2}\pi\alpha_s \mathbf{p}_T^2. \tag{2}$$

Neglecting quark masses, the effective $\mathcal{Q}\overline{\mathcal{Q}}\gamma$ and $\mathcal{Q}\overline{\mathcal{Q}}g$ vertices read [20]:

$$C^{\gamma/g,\mu}_{\mathcal{Q}\overline{\mathcal{Q}}}(q_1, q_2) = C_1^{\gamma/g} \left[\gamma^\mu - \not{q}_1 \frac{(n^-)^\mu}{q_1^- + q_2^-} - \not{q}_2 \frac{(n^+)^\mu}{q_1^+ + q_2^+} \right], \tag{3}$$

where $C_1^\gamma = -i\sqrt{4\pi\alpha} e_q$, with α being Sommerfeld's fine-structure constant and e_q being the fractional charge of quark q (and its Reggeized variant $\mathcal{Q}$), and $C_1^g = -i\sqrt{4\pi\alpha_s} T^a$, with T^a being a generator of SU(3). The squared amplitudes of the partonic subprocesses $\mathcal{Q}\overline{\mathcal{Q}} \to \gamma$ and $\mathcal{Q}\overline{\mathcal{Q}} \to g$ are found from Eq. (3) to be

$$\overline{\left| \mathcal{M}\left(\mathcal{Q} + \overline{\mathcal{Q}} \to \gamma/g \right) \right|^2} = C_2^{\gamma/g}(t_1 + t_2), \tag{4}$$

where $C_2^\gamma = (4/3)\pi\alpha e_q^2$ and $C_2^g = (16/3)\pi\alpha_s$.

III. CROSS SECTIONS

Exploiting the hypothesis of high-energy factorization, we may write the hadronic cross sections $d\sigma$ as convolutions of partonic cross sections $d\hat{\sigma}$ with unintegrated PDFs Φ_a^h of

Reggeized partons a in the hadrons h, as

$$d\sigma\left(p\overline{p}\to j+X\right)=\int\frac{dx_1}{x_1}\int\frac{d^2q_{1T}}{\pi}\int\frac{dx_2}{x_2}\int\frac{d^2q_{2T}}{\pi}\Phi_g^p(x_1,t_1,\mu^2)\Phi_g^{\overline{p}}(x_2,t_2,\mu^2)d\hat{\sigma}\left(\mathcal{R}\mathcal{R}\to g\right), \tag{5}$$

and similarly for pp collisions and single prompt-photon production. For the reader's convenience, we also present here a compact formula for the double differential distribution in $p_T=|\mathbf{p_T}|$ and y, which follows from Eq. (5) and reads:

$$\frac{d\sigma}{dp_T\,dy}\left(p\overline{p}\to j+X\right)=\frac{1}{p_T^3}\int d\phi_1\int dt_1\Phi_g^p(x_1,t_1,\mu^2)\Phi_g^{\overline{p}}(x_2,t_2,\mu^2)\overline{\left|\mathcal{M}\left(\mathcal{R}\mathcal{R}\to g\right)\right|^2}, \tag{6}$$

where ϕ_1 is the azimuthal angle enclosed between $\mathbf{q}_{1T}$ and $\mathbf{p}_T$,

$$x_{1,2}=\frac{p_T\exp(\pm y)}{\sqrt{S}},\qquad t_2=t_1+p_T^2-2p_T\sqrt{t_1}\cos\phi_1. \tag{7}$$

In the case of single prompt-photon inclusive production, we take the first three quark flavors, u, d, and s, to be active. Since we work at LO, the produced jet has zero invariant mass m, so that transverse energy $E_T=\sqrt{p_T^2+m^2}$ and transverse momentum p_T coincide and so do rapidity $y=(1/2)\ln[(p^0+p^3)/(p^0-p^3)]$ and pseudorapidity $\eta=-\ln\tan(\theta/2)$, where θ is the angle enclosed between the jet and beam axes.

The unintegrated PDFs $\Phi_a^h(x,t,\mu^2)$ are related to their collinear counterparts $F_a^h(x,\mu^2)$ by the normalization condition,

$$xF_a^h(x,\mu^2)=\int^{\mu^2}dt\,\Phi_a^h(x,t,\mu^2), \tag{8}$$

which yields the correct transition from formulas in the QMRK approach to those in the collinear parton model, where the transverse momenta of the partons are neglected. In our numerical analysis, we adopt as our default the prescription proposed by Kimber, Martin, and Ryskin (KMR) [21] to obtain unintegrated gluon and quark PDFs of the proton from the conventional integrated ones, as implemented in Watt's code [22]. As is well known [23], other popular prescriptions, such as those by Blümlein (B) [24] or by Jung and Salam [25], produce unintegrated PDFs with distinctly different t dependences. In order to assess the resulting theoretical uncertainty, we also evaluate the unintegrated gluon PDF using the B approach, which resums small-x effects according to the BFKL equation. As input for these procedures, we use the LO set of the Martin-Roberts-Stirling-Thorne (MRST) [26] proton PDFs as our default. In order to estimate the theoretical uncertainty due to the freedom in

the choice of the PDFs, we also use the CTEQ6L1 set by the CTEQ Collaboration [27] as well as the Glück-Reya-Vogt (GRV) [28] LO set.

Throughout our analysis the renormalization and factorization scales are identified and chosen to be $\mu = \xi p_T$, where ξ is varied between 1/2 and 2 about its default value 1 to estimate the theoretical uncertainty due to the freedom in the choice of scales. The resulting errors are indicated as shaded bands in the figures.

IV. RESULTS

We are now in a position to present our theoretical predictions and to compare them with experimental measurements. We first consider single jet inclusive production. Recently, the CDF [13] (D0 [14]) Collaboration presented new data from Tevatron run II, which correspond to an integrated luminosity of 1.13 fb^{-1} (0.70 fb^{-1}) and cover the kinematic range 62 GeV $< p_T <$ 700 GeV (50 GeV $< p_T <$ 600 GeV) and $|y| < 2.1$ ($|y| < 2.4$). The CDF and D0 data are compared with our MRK predictions in Figs. 1 and 2, respectively. We find good agreement for $p_T \lesssim 100$ GeV, which corresponds to $x_T \lesssim 0.1$, while our default predictions overshoot the data for larger values of p_T. This may be understood by observing that the average values of the scaling variables x_1 and x_2 in Eq. (6) are of order x_T, and the MRK picture ceases to be valid for $x_i \gtrsim 0.1$. For $x_T \gtrsim 0.1$, one needs to resort to the collinear parton model, which starts with $2 \to 2$ partonic subprocesses at LO. Since the unintegrated quark PDFs are greatly suppressed compared to the gluon one, the contributions due to partonic subprocesses involving Reggeized quarks, such as $\mathcal{R}\mathcal{Q} \to q$ and $\mathcal{Q}\overline{\mathcal{Q}} \to g$, are expected to be relatively small in the relevant x_T range, $x_T \gtrsim 0.1$. The predictions obtained using the B approach undershoot the default ones leading to a better description of the experimental data at large values of p_T, where the MRK picture is, however, not expected to apply. However, they undershoot the experimental data at large values of $|y|$ throughout the whole p_T range considered.

In Figs. 1 and 2, the theoretical uncertainties due to the fredom in the choices of the renormalization and factorization scales are indicated for the default predictions by the shaded bands. Our limited knowledge of the unintegrated PDFs also contributes to the theoretical uncertainty. In Figs. 3 and 4, we investigate this source of theoretical uncertainty for the p_T distribution of single jet inclusive hadroproduction in $p\overline{p}$ collisions with $\sqrt{S} =$

1.96 TeV integrated over the rapidity intervals $|y| < 0.1$ and $1.6 < |y| < 2.1$, respectively. Specifically, we consider the evaluations, for $\xi = 1$, with the CTEQ6L1 [27] and GRV LO [28] PDFs normalized to the ones with the MRST LO PDFs [26]. These ratios are typically well contained within the bands generated by varying ξ between 1/2 and 2 in the evaluations with the MRST LO PDFs. We thus conclude that scale variations provide reasonable estimates of the overall theoretical uncertainties in the evaluations based on the KMR approach.

Moving on from the Tevatron to the LHC, which is currently running at $\sqrt{S} = 7$ TeV, being about 3.5 larger than at the Tevatron, one expects the p_T range of validity of the MRK picture to be extended by the same factor, to $p_T \lesssim 350$ GeV. This expectation is nicely confirmed in Figs. 5 and 6, where a recent measurement by the ATLAS Collaboration [17], which is based on an integrated luminosity of 17 nb^{-1} and covers the kinematic range 60 GeV $< p_T <$ 600 GeV and $|y| < 2.8$, is compared with our MRK predictions for the p_T and y distributions, respectively. In fact, useful agreement is found even through the largest p_T values accessed by this measurement.

Note that, in Ref. [17], jets are identified using the anti-k_t jet-clustering algorithm with two different values of the jet-size parameter $R = \sqrt{(\Delta y)^2 + (\Delta\phi)^2}$, namely $R = 0.4$ and $R = 0.6$. The ATLAS data shown in Figs. 5 and 6 refer to $R = 0.6$. The agreement is somewhat worse for $R = 0.4$. This may be understood by observing that the MRK picture assumes a strong hierarchy in y and thus prefers a stronger isolation. Our LO prediction does not yet depend on R.

In Figs. 7 and 8, we repeat the MRK analyses of Figs. 5 and 6 for the LHC design c.m. energy $\sqrt{S} = 14$ TeV, where we expect the p_T range of validity to be roughly $p_T \lesssim 700$ GeV.

Let us now turn to single prompt-photon inclusive production. In Figs. 9 and 10, we compare our MRK predictions with data taken by the D0 Collaboration in Tevatron runs I [15] and II [16], respectively. The analysis of Ref. [15] ([16]) is based on an integrated luminosity of 107.6 pb^{-1} (326 pb^{-1}) and covers the kinematic range 10 GeV $< E_T <$ 140 GeV (23 GeV $< p_T <$ 300 GeV) and $|\eta| < 2.5$ ($|\eta| < 0.9$). We find reasonable agreement through $E_T \approx 85$ GeV ($p_T \approx 60$ GeV) for the central events, with $|\eta| < 0.9$, from run I [15] (run II [16]), but only through $p_T \approx 36$ GeV for the forward events, with $1.6 < |\eta| < 0.9$, from run I [15]. Fragmentation production, via partonic subprocesses such as $\mathcal{R}\mathcal{Q} \to q \to \gamma$ and $\mathcal{R}\mathcal{R} \to g \to \gamma$, should be numerically small compared to direct production and is neglected in our exploratory analysis.

In Fig. 11, we compare our MRK predictions with a very recent measurement by the ATLAS Collaboration, which is based on an integrated luminosity of 880 nb^{-1} and covers the kinematic range 15 GeV $< p_T <$ 100 GeV and $|\eta| < 1.81$. The agreement is found to be excellent, as expected because of the small x_T values probed.

Finally, we repeat the MRK analyses of Fig. 11 for $\sqrt{S} = 14$ TeV and show the results in Fig. 12.

V. CONCLUSIONS

The Tevatron and, even more so, the LHC are currently probing particle physics at terascale c.m. energies $\sqrt{S}$, so that the hierarchy $\Lambda_{\text{QCD}} \ll \mu \ll \sqrt{S}$, which defines the MRK regime, is satisfied for a wealth of QCD processes of typical energy scale μ.

In this paper, we studied two QCD processes of particular interest, namely single jet and prompt-photon inclusive hadroproduction, at LO in the MRK approach, in which they are mediated by $2 \to 1$ partonic subprocesses initiated by Reggeized gluons and quarks, respectively. Despite the great simplicity of our analytic expressions, we found excellent agreement with single jet [17] and prompt-photon [18] data taken just recently by the ATLAS Collaboration in pp collisions with $\sqrt{S} = 7$ TeV at the LHC. By contrast, in the collinear parton model of QCD, it is necessary to take into account NLO corrections and to perform soft-gluon resummation in order to obtain a comparable degree of agreement with the data, both for jet [29] and prompt-photon [30] inclusive production. However, our findings have to be taken with a grain of salt, since our LO approach does not yet accommodate the concepts of single-jet cone radius and prompt-photon isolation cone and neglects fragmentation to prompt photons.

On the other hand, comparisons with data taken by the CDF and D0 Collaborations at the Tevatron in $p\overline{p}$ collisons with $\sqrt{S} = 1.8$ TeV and 1.96 TeV, which is roughly a factor of 3.5 below the value presently reached by the LHC, disclosed the limits of applicability of the MRK picture. In fact, the MRK approximation appears to break down for $x_T \gtrsim 0.1$ in the case of single jet production and somewhat below that in the case of single prompt-photon production.

These findings are in line with our previous studies of the MRK approach, applied to the production of prompt photons [7], diphotons [8], charmed mesons [9], bottom-flavored jets

[10], charmonia [11], and bottomonia [12]. Here and in Refs. [7–12], parton Reggeization was demonstrated to be a powerful tool for the theoretical description of QCD processes in the high-energy limit.

VI. ACKNOWLEDGEMENTS

We are grateful to V. S Fadin and L. N. Lipatov for useful discussions. This research was supported in part by the German Federal Ministry for Education and Research BMBF under Grant No. 05 HT6GUA, by the Helmholtz Association HGF under Grant No. Ha 101, by the National Science Foundation NSF under Grant No. NSF PHY05-51164, and by the Claussen-Simon-Stiftung. The work of V.A.S. and A.V.S. was supported in part by the Federal Ministry for Science and Education of the Russian Federation under Contract No. 14.740.11.0894. A.V.S. is grateful to the International Center of Fundamental Physics in Moscow and the Dynastiya Foundation for financial support. The work of E.V.Y. was supported in part by Michail Lomonosov Grant No. A/09/72753, jointly funded by the German Academic Exchange Service DAAD and the Ministry of Science and Education of the Russian Federation.

---

[1] V. T. Kim and G. B. Pivovarov, Phys. Rev. D **57**, 1341 (1998) [arXiv:hep-ph/9709433].

[2] L. N. Lipatov, Sov. J. Nucl. Phys. **23**, 338 (1976) [Yad. Fiz. **23**, 642 (1976)]; E. A. Kuraev, L. N. Lipatov, and V. S. Fadin, Sov. Phys. JETP **44**, 443 (1976) [Zh. Eksp. Teor. Fiz. **71**, 840 (1976)]; Sov. Phys. JETP **45**, 199 (1977) [Zh. Eksp. Teor. Fiz. **72**, 377 (1977)]; I. I. Balitsky and L. N. Lipatov, Sov. J. Nucl. Phys. **28**, 822 (1978) [Yad. Fiz. **28**, 1597 (1978)]; Sov. Phys. JETP **63**, 904 (1986) [Zh. Eksp. Teor. Fiz. **90**, 1536 (1986)].

[3] D. Ostrovsky, Phys. Rev. D **62**, 054028 (2000) [arXiv:hep-ph/9912258].

[4] V. S. Fadin and L. N. Lipatov, Nucl. Phys. **B406**, 259 (1993); **B477**, 767 (1996) [arXiv:hep-ph/9602287].

[5] L. N. Lipatov, Nucl. Phys. **B452**, 369 (1995) [arXiv:hep-ph/9502308].

[6] L. N. Lipatov and M. I. Vyazovsky, Nucl. Phys. **B597**, 399 (2001) [arXiv:hep-ph/0009340].

[7] V. A. Saleev, Phys. Rev. D **78**, 034033 (2008) [arXiv:0807.1587 [hep-ph]]; Phys. Rev. D **78**,

114031 (2008) [arXiv:0812.0946 [hep-ph]].

[8] V. A. Saleev, Phys. Rev. D **80**, 114016 (2009) [arXiv:0911.5517 [hep-ph]].

[9] B. A. Kniehl, A. V. Shipilova, and V. A. Saleev, Phys. Rev. D **79**, 034007 (2009) [arXiv:0812.3376 [hep-ph]].

[10] B. A. Kniehl, V. A. Saleev, and A. V. Shipilova, Phys. Rev. D **81**, 094010 (2010) [arXiv:1003.0346 [hep-ph]]; PoS(DIS2010), 177 (2010); in Proceedings of Physics at the LHC 2010 (PLHC2010), Hamburg, Germany, 2010, edited by M. Diehl, J. Haller, T. Schörner-Sadenius, and G. Steinbrueck, DOI: `http://dx.doi.org/10.3204/DESY-PROC-2010-01/shipilova`.

[11] B. A. Kniehl, D. V. Vasin, and V. A. Saleev, Phys. Rev. D **73**, 074022 (2006) [arXiv:hep-ph/0602179]; in Proceedings of the 15th International Workshop on Deep-Inelastic Scattering and Related Subjects (DIS 2007), Munich, Germany, 2007, edited by G. Grindhammer and K. Sachs, DOI: `http://dx.doi.org/10.3360/dis.2007.169`.

[12] B. A. Kniehl, V. A. Saleev, and D. V. Vasin, Phys. Rev. D **74**, 014024 (2006) [arXiv:hep-ph/0607254].

[13] CDF Collaboration, T. Aaltonen *et al.*, Phys. Rev. D **78**, 052006 (2008); **79**, 119902(E) (2009) [arXiv:0807.2204 [hep-ex]].

[14] D0 Collaboration, V. M. Abazov *et al.*, Phys. Rev. Lett. **101**, 062001 (2008) [arXiv:0802.2400 [hep-ex]].

[15] D0 Collaboration, B. Abbott *et al.*, Phys. Rev. Lett. **84**, 2786 (2000) [arXiv:hep-ex/9912017].

[16] D0 Collaboration, V. M. Abazov *et al.*, Phys. Lett. B **639**, 151 (2006); **658**, 285(E) (2008) [arXiv:hep-ex/0511054].

[17] ATLAS Collaboration, G. Aad *et al.*, Eur. Phys. J. C **71**, 1512 (2011) [arXiv:1009.5908 [hep-ex]].

[18] ATLAS Collaboration, G. Aad *et al.*, Phys. Rev. D **83**, 052005 (2011) [arXiv:1012.4389 [hep-ex]].

[19] V. S. Fadin and L. N. Lipatov, JETP Lett. **49**, 352 (1989) [Pis'ma Zh. Eksp. Teor. Fiz. **49**, 311 (1989)]; Sov. J. Nucl. Phys. **50**, 712 (1989) [Yad. Fiz. **50**, 1141 (1989)]; E. N. Antonov, L. N. Lipatov, E. A. Kuraev, and I. O. Cherednikov, Nucl. Phys. **B721**, 111 (2005) [arXiv:hep-ph/0411185].

[20] V. S. Fadin and V. E. Sherman, JETP Lett. **23**, 548 (1976) [Pis'ma Zh. Eksp. Teor. Fiz. **23**,

599 (1976)]; Sov. Phys. JETP **45**, 861 (1977) [Zh. Eksp. Teor. Fiz. **72**, 1640 (1977)].

[21] M. A. Kimber, A. D. Martin, and M. G. Ryskin, Eur. Phys. J. C **12**, 655 (2000) [arXiv:hep-ph/9911379]; Phys. Rev. D **63**, 114027 (2001) [arXiv:hep-ph/0101348]; G. Watt, A. D. Martin, and M. G. Ryskin, Eur. Phys. J. C **31**, 73 (2003) [arXiv:hep-ph/0306169]; Phys. Rev. D **70**, 014012 (2004); **70**, 079902(E) (2004) [arXiv:hep-ph/0309096].

[22] G. Watt, URL: `http://gwatt.web.cern.ch/gwatt/`.

[23] Small-x Collaboration, B. Andersson *et al.*, Eur. Phys. J. C **25**, 77 (2002) [arXiv:hep-ph/0204115]; F. Hautmann and H. Jung, Nucl. Phys. B (Proc. Suppl.) **184**, 64 (2008) [arXiv:0712.0568 [hep-ph]].

[24] J. Blümlein, Preprint DESY 95–121 (1995) [arXiv:hep-ph/9506403].

[25] H. Jung and G. P. Salam, Eur. Phys. J. C **19**, 351 (2001) [arXiv:hep-ph/0012143].

[26] A. D. Martin, R. G. Roberts, W. J. Stirling, and R. S. Thorne, Phys. Lett. B **531**, 216 (2002) [arXiv:hep-ph/0201127].

[27] J. Pumplin, D. R. Stump, J. Huston, H.-L. Lai, P. M. Nadolsky, and W.-K. Tung, JHEP **0207**, 012 (2002) [arXiv:hep-ph/0201195]; D. Stump, J. Huston, J. Pumplin, W.-K. Tung, H.-L. Lai, S. Kuhlmann, and J. F. Owens, JHEP **0310**, 046 (2003) [arXiv:hep-ph/0303013].

[28] M. Glück, E. Reya, and A. Vogt, Z. Phys. C **67**, 433 (1995).

[29] F. Aversa, P. Chiappetta, M. Greco, and J. Ph. Guillet, Phys. Lett. B **210**, 225 (1988); **211**, 465 (1988); Nucl. Phys. **B327**, 105 (1989); Z. Phys. C **46**, 253 (1990); Phys. Rev. Lett. **65**, 401 (1990); S. D. Ellis, Z. Kunszt, and D. E. Soper, Phys. Rev. Lett. **62**, 726 (1989); Phys. Rev. D **40**, 2188 (1989); Phys. Rev. Lett. **64**, 2121 (1990); N. Kidonakis, Int. J. Mod. Phys. A **15**, 1245 (2000) [arXiv:hep-ph/9902484]; A. Banfi, G. P. Salam, and G. Zanderighi, JHEP **1006**, 038 (2010) [arXiv:1001.4082 [hep-ph]].

[30] P. Aurenche, R. Baier, M. Fontannaz, and D. Schiff, Nucl. Phys. B **297**, 661 (1988); L. E. Gordon and W. Vogelsang, Phys. Rev. D **50**, 1901 (1994); J. Huston, E. Kovacs, S. Kuhlmann, H. L. Lai, J. F. Owens, and W. K. Tung, Phys. Rev. D **51**, 6139 (1995) [arXiv:hep-ph/9501230]; P. Aurenche, M. Fontannaz, J. Ph. Guillet, B. Kniehl, E. Pilon, and M. Werlen, Eur. Phys. J. C **9**, 107 (1999) [arXiv:hep-ph/9811382]; S. Catani, M. L. Mangano, P. Nason, C. Oleari, and W. Vogelsang, JHEP **9903**, 025 (1999) [arXiv:hep-ph/9903436]; N. Kidonakis and J. F. Owens, Phys. Rev. D **61**, 094004 (2000) [arXiv:hep-ph/9912388]; P. Bolzoni, S. Forte, and G. Ridolfi, Nucl. Phys. **B731**, 85 (2005) [arXiv:hep-ph/0504115]; D. de Florian and W. Vogelsang, Phys.

Rev. D **72**, 014014 (2005) [arXiv:hep-ph/0506150]; G. Diana, Nucl. Phys. **B824**, 154 (2010) [arXiv:0906.4159 [hep-ph]]; G. Diana, J. Rojo, and R. D. Ball, Phys. Lett. B **693**, 430 (2010) [arXiv:1006.4250 [hep-ph]].

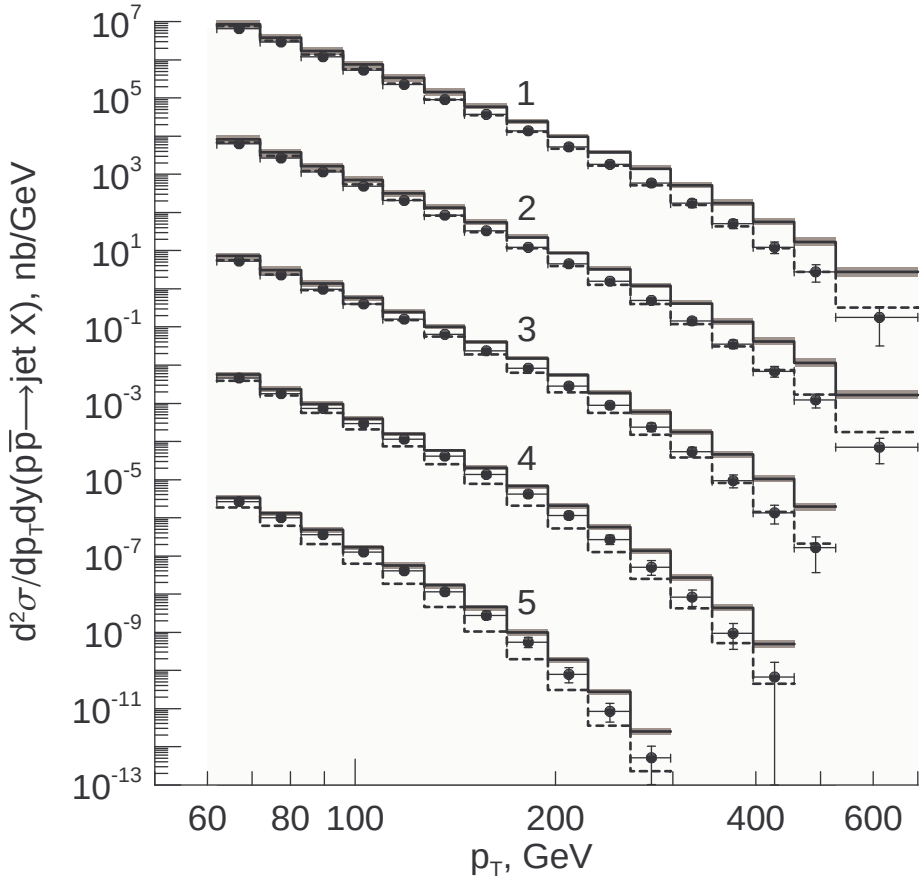

FIG. 1: The transverse-momentum distributions of single jet inclusive hadroproduction measured in the rapidity intervals (1) $|y| < 0.1$ ($\times 10^6$), (2) $0.1 < |y| < 0.7$ ($\times 10^3$), (3) $0.7 < |y| < 1.1$, (4) $1.1 < |y| < 1.6$ ($\times 10^{-3}$), and (5) $1.6 < |y| < 2.1$ ($\times 10^{-6}$) by the CDF Collaboration in Tevatron run II [13] are compared with our LO MRK predictions evaluated in the KMR (solid histograms) and B (dashed histograms) approaches using the MRST PDFs. The shaded bands indicate the scale uncertainties in the KMR evaluations.

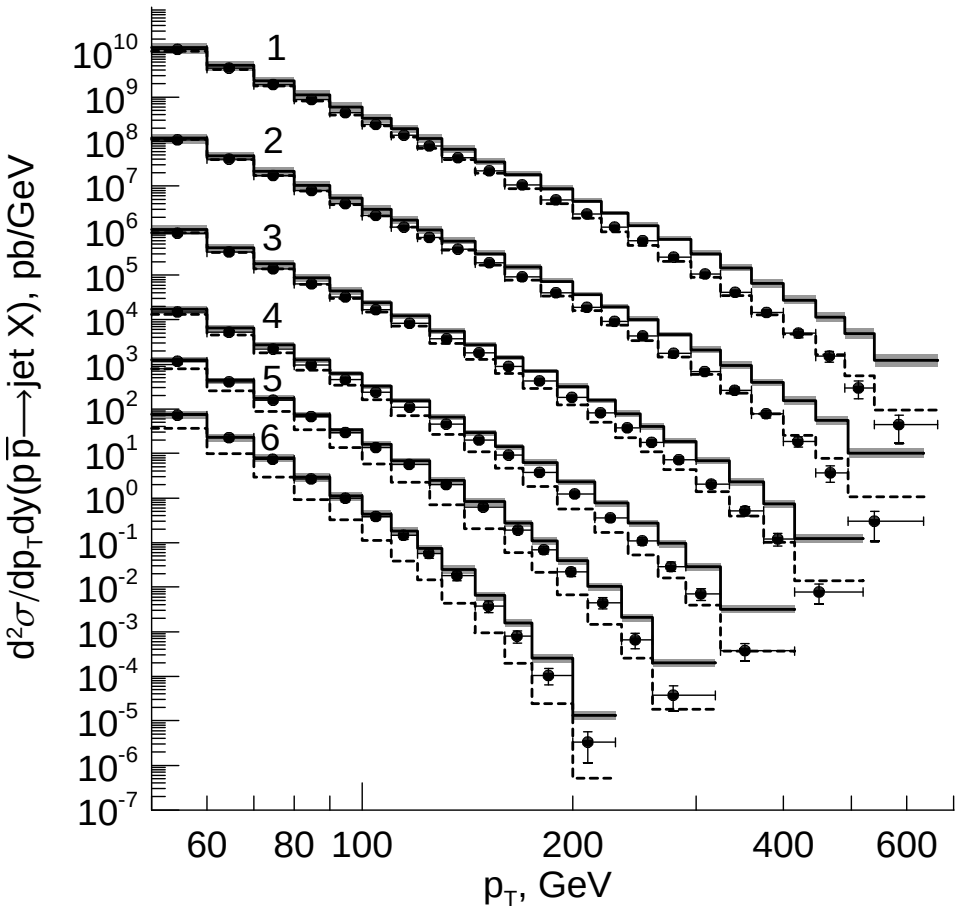

FIG. 2: The transverse-momentum distributions of single jet inclusive hadroproduction measured in the rapidity intervals (1) $|y| < 0.4$ ($\times 5 \cdot 10^5$), (2) $0.4 < |y| < 0.8$ ($\times 5 \cdot 10^3$), (3) $0.8 < |y| < 1.2$ ($\times 50$), (4) $1.2 < |y| < 1.6$, (5) $1.6 < |y| < 2.0$ ($\times 0.1$), and (6) $2.0 < |y| < 2.4$ ($\times 10^{-2}$) by the D0 Collaboration in Tevatron run II [14] are compared with our LO MRK predictions evaluated in the KMR (solid histograms) and B (dashed histograms) approaches using the MRST PDFs. The shaded bands indicate the scale uncertainties in the KMR approach.

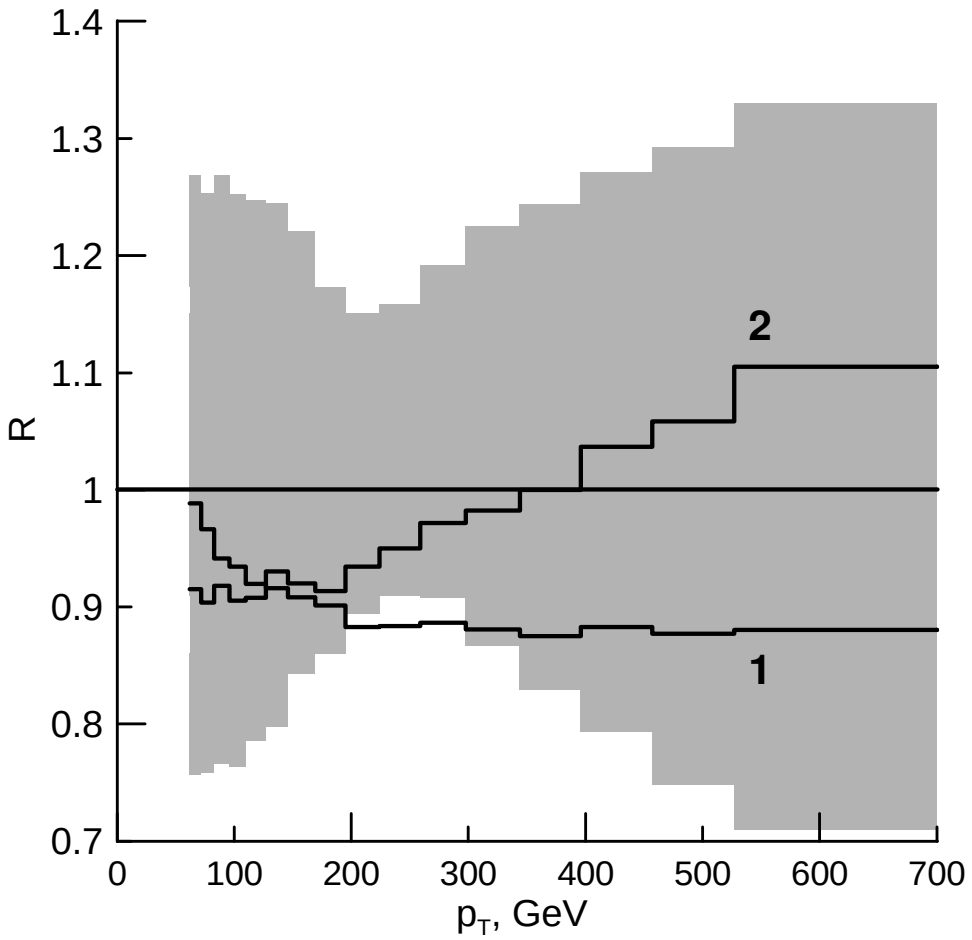

FIG. 3: Theoretical uncertainties in the KMR approach due to the freedom in the choices of scales and unintegrated PDF set in the transverse-momentum distribution of single jet inclusive hadroproduction in $p\overline{p}$ collisions with $\sqrt{S} = 1.96$ TeV integrated over the rapidity interval $|y| < 0.1$. The evaluation with the MRST LO set and ξ varied in the interval $1/2 < \xi < 2$ (shaded band) and those with the (1) CTEQ6L1 and (2) GRV LO sets and $\xi = 1$ are normalized to the one with the MRST LO set and $\xi = 1$.

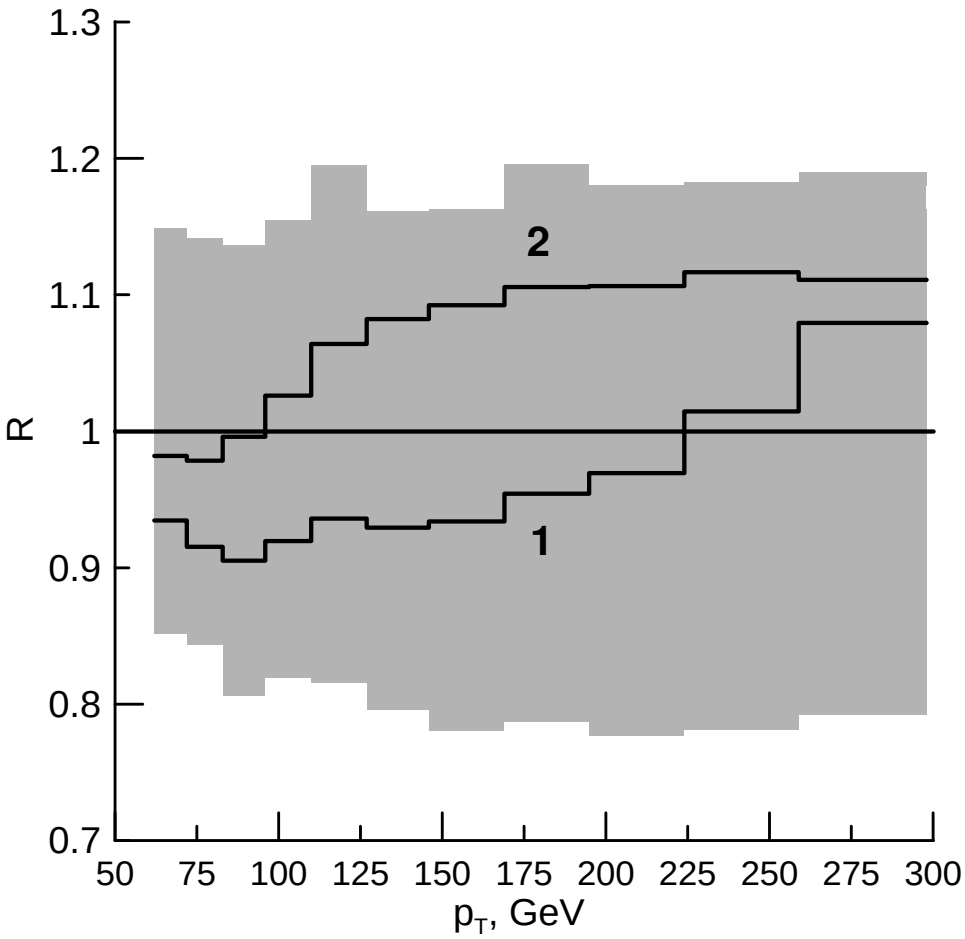

FIG. 4: Theoretical uncertainties in the KMR approach due to the freedom in the choices of scales and unintegrated PDF set in the transverse-momentum distribution of single jet inclusive hadroproduction in $p\overline{p}$ collisions with $\sqrt{S} = 1.96$ TeV integrated over the rapidity interval $1.6 < |y| < 2.1$. The evaluation with the MRST LO set and ξ varied in the interval $1/2 < \xi < 2$ (shaded band) and those with the (1) CTEQ6L1 and (2) GRV LO sets and $\xi = 1$ are normalized to the one with the MRST LO set and $\xi = 1$.

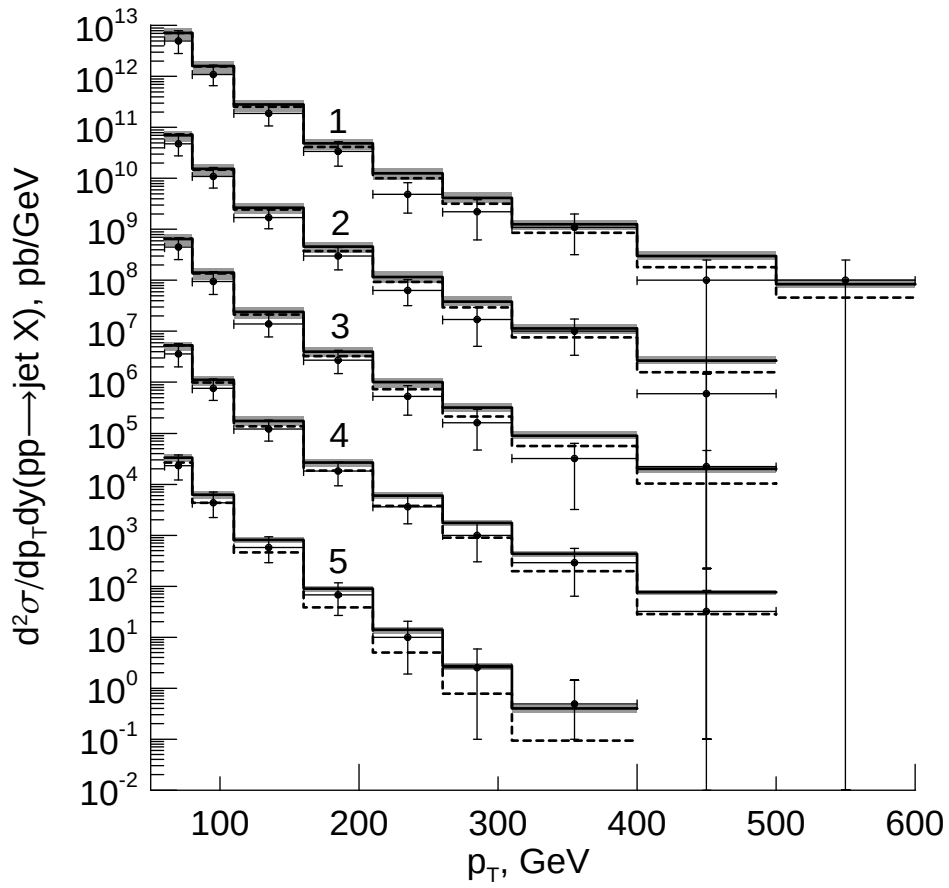

FIG. 5: The transverse-momentum distributions of single jet inclusive hadroproduction measured in the rapidity intervals (1) $|y| < 0.3$ ($\times 10^8$), (2) $0.3 < |y| < 0.8$ ($\times 10^6$), (3) $0.8 < |y| < 1.2$ ($\times 10^4$), (4) $1.2 < |y| < 2.1$ ($\times 10^2$), and (5) $2.1 < |y| < 2.6$ by the ATLAS Collaboration at the LHC [17] are compared with our LO MRK predictions evaluated in the KMR (solid histograms) and B (dashed histograms) approaches using the MRST PDFs. The shaded bands indicate the scale uncertainties in the KMR evaluations.

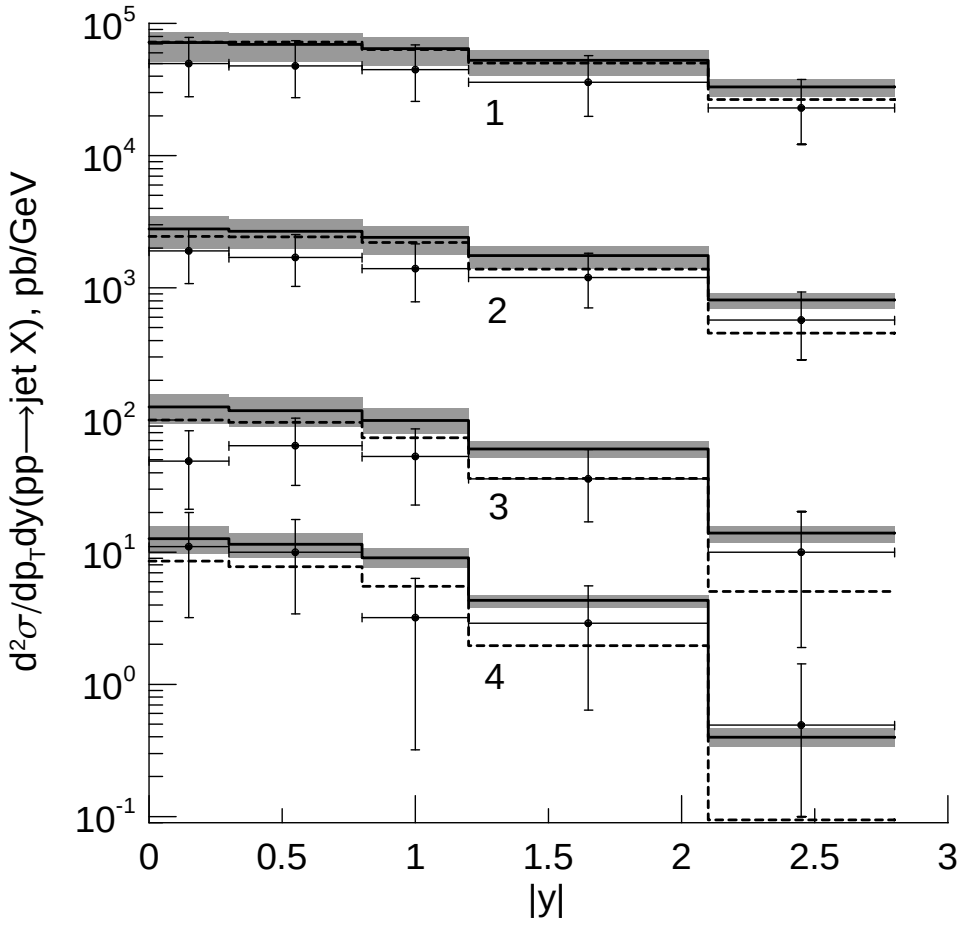

FIG. 6: The rapidity distributions of single jet inclusive hadroproduction measured in the transverse-momentum intervals (1) 60 GeV $< p_T <$ 80 GeV, (2) 110 GeV $< p_T <$ 160 GeV, (3) 210 GeV $< p_T <$ 250 GeV, and (4) 310 GeV $< p_T <$ 400 GeV by the ATLAS Collaboration at the LHC [17] are compared with our LO MRK predictions evaluated in the KMR (solid histograms) and B (dashed histograms) approaches using the MRST PDFs. The shaded bands indicate the scale uncertainties in the KMR evaluations.

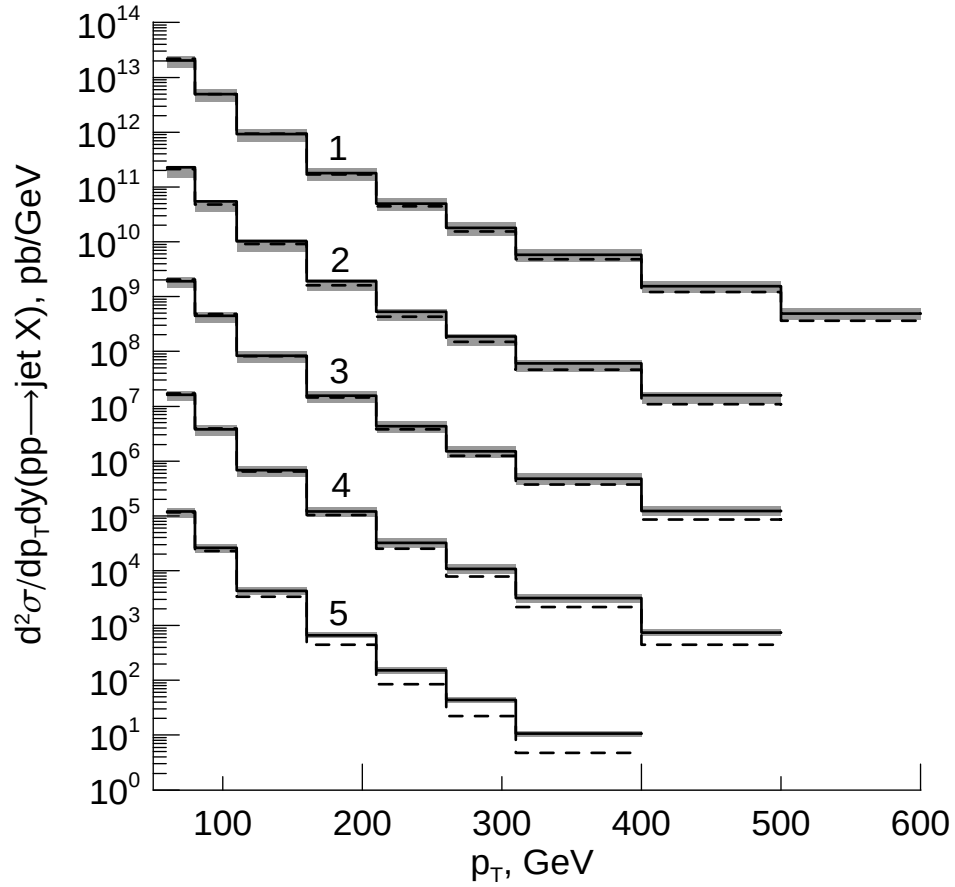

FIG. 7: Transverse-momentum distributions of single jet inclusive hadroproduction in pp collisions with $\sqrt{S} = 14$ TeV integrated over the rapidity intervals (1) $|y| < 0.3$ ($\times 10^8$), (2) $0.3 < |y| < 0.8$ ($\times 10^6$), (3) $0.8 < |y| < 1.2$ ($\times 10^4$), (4) $1.2 < |y| < 2.1$ ($\times 10^2$), and (5) $2.1 < |y| < 2.6$ as predicted at LO in the MKR framework adopting the KMR (solid histograms) and B (dashed histograms) approaches with the MRST PDFs. The shaded bands indicate the scale uncertainties in the KMR evaluations.

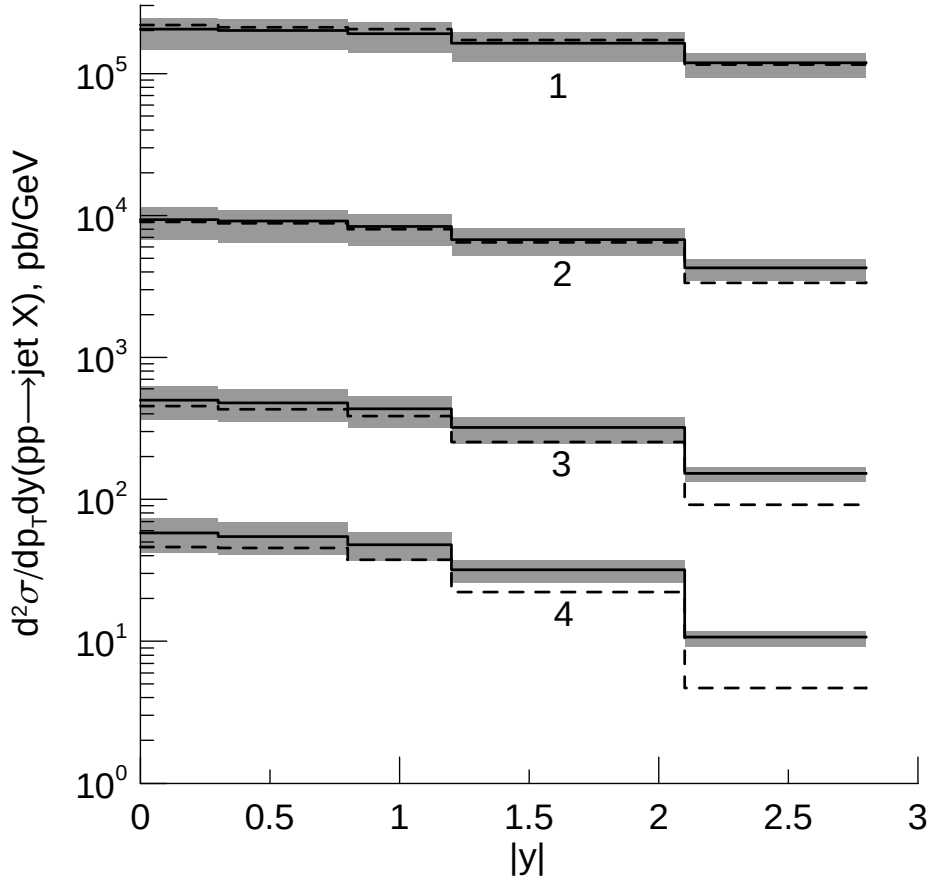

FIG. 8: Rapidity distributions of single jet inclusive hadroproduction in pp collisions with $\sqrt{S} =$ 14 TeV integrated over the transverse-momentum intervals (1) 60 GeV $< p_T <$ 80 GeV, (2) 110 GeV $< p_T <$ 160 GeV, (3) 210 GeV $< p_T <$ 250 GeV, and (4) 310 GeV $< p_T <$ 400 GeV as predicted at LO in the MKR framework adopting the KMR (solid histograms) and B (dashed histograms) approaches with the MRST PDFs. The shaded bands indicate the scale uncertainties in the KMR evaluations.

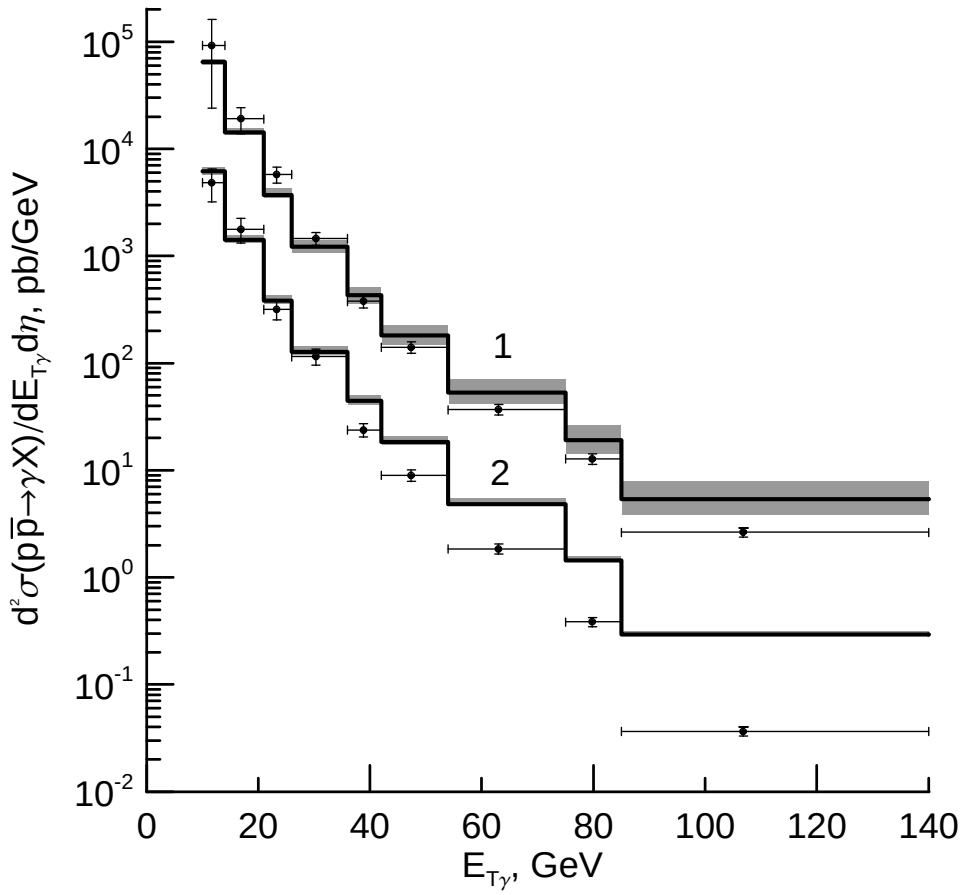

FIG. 9: The transverse-energy distributions of single prompt-photon inclusive hadroproduction measured in the pseudorapidity intervals (1) $|\eta| < 0.9$ ($\times 10$) and (2) $1.6 < |\eta| < 2.5$ by the D0 Collaboration in Tevatron run I [15] are compared with our LO MRK predictions. The shaded bands indicate the theoretical uncertainties.

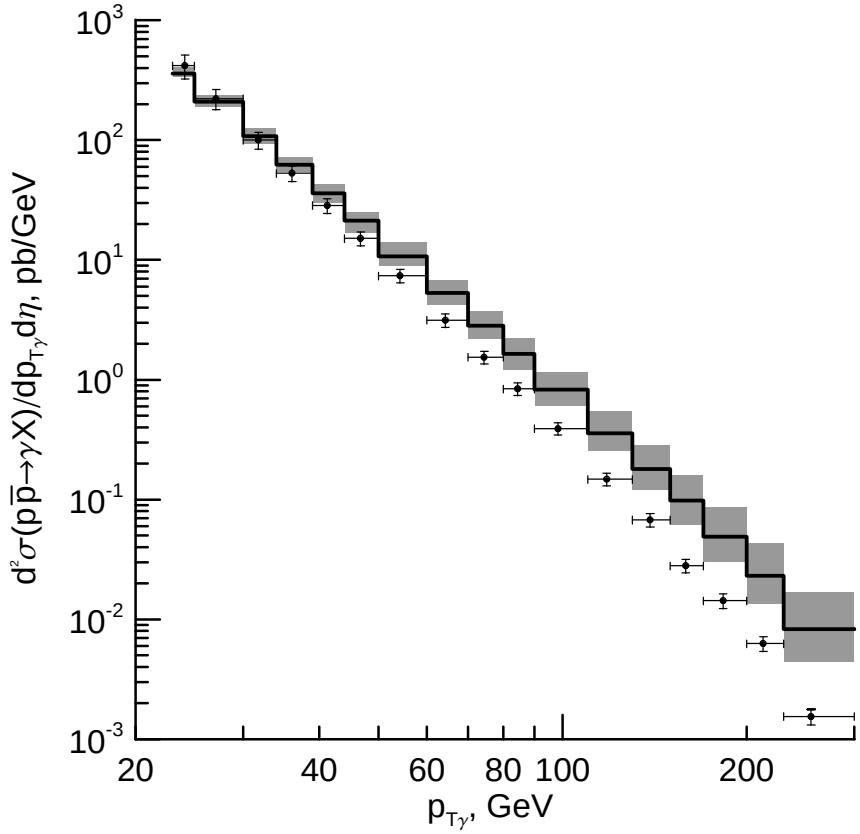

FIG. 10: The transverse-momentum distribution of single prompt-photon inclusive hadroproduction measured in the pseudorapidity interval $|\eta| < 0.9$ by the D0 Collaboration in Tevatron run II [16] is compared with our LO MRK predictions. The shaded band indicates the theoretical uncertainty.

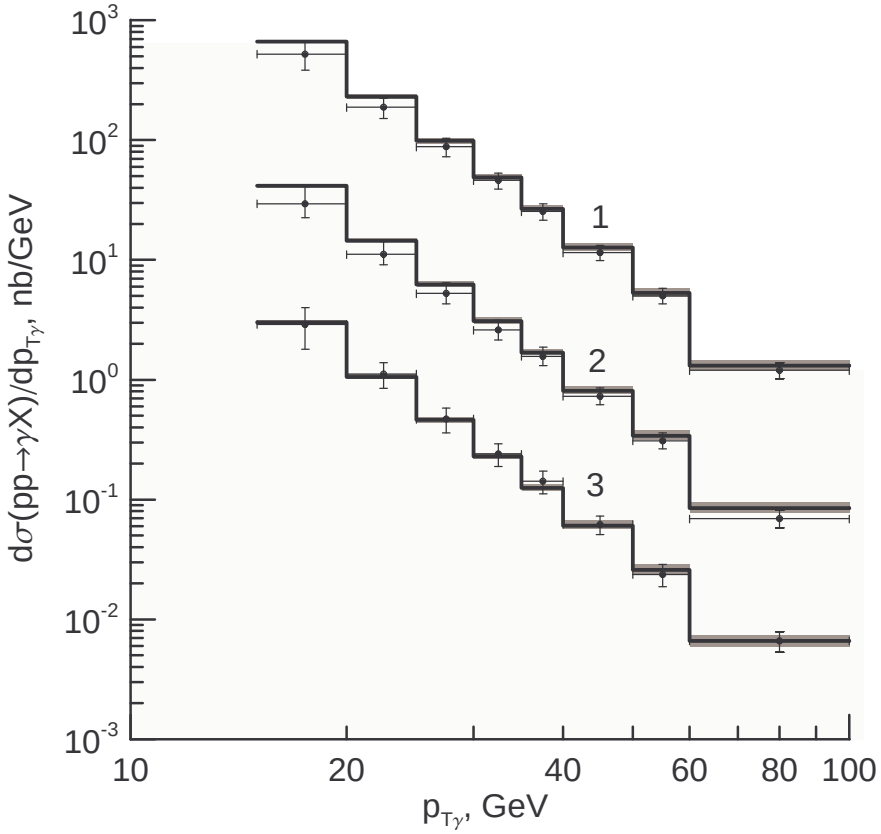

FIG. 11: The transverse-momentum distributions of single prompt-photon inclusive hadroproduction measured in the pseudorapidity intervals (1) $|\eta| < 0.6$ ($\times 10^2$), (2) $0.6 < |\eta| < 1.37$ ($\times 5$), and (3) $1.52 < |\eta| < 1.81$ by the ATLAS Collaboration at the LHC [17] are compared with our LO MRK predictions. The shaded bands indicate the theoretical uncertainties.

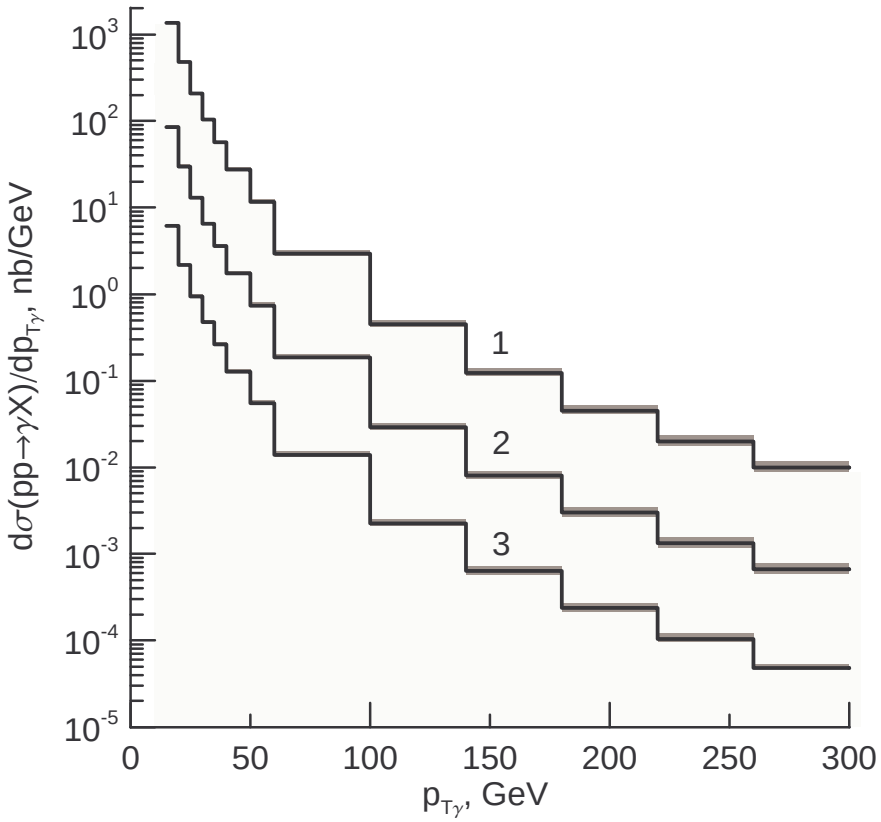

FIG. 12: Transverse-momentum distributions of single prompt-photon inclusive hadroproduction in pp collisions with $\sqrt{S} = 14$ TeV integrated over the pseudorapidity intervals (1) $|\eta| < 0.6$ ($\times 10^2$), (2) $0.6 < |\eta| < 1.37$ ($\times 5$), and (3) $1.52 < |\eta| < 1.81$ as predicted at LO in the MKR approach. The shaded bands indicate the theoretical uncertainties.